

Multi-Resolution POMDP Planning for Multi-Object Search in 3D

Kaiyu Zheng¹, Yoonchang Sung², George Konidaris¹, Stefanie Tellex¹

Abstract— Robots operating in household environments must find objects on shelves, under tables, and in cupboards. Previous work often formulates the object search problem as a POMDP (Partially Observable Markov Decision Process), yet constrain the search space in 2D to reduce computational complexity, although objects exist in a rich 3D environment. We present a POMDP formulation for multi-object search in a 3D region with a frustum-shaped field-of-view and an efficient multi-resolution planning algorithm to solve this POMDP. To achieve efficient planning, our algorithm uses a new octree-based representation that captures beliefs at different resolution levels, enabling the agent to induce abstract POMDPs with dramatically smaller state and observation spaces. Our evaluation in a simulated 3D domain shows that our approach achieves significantly higher reward ($\geq 51\%$ in the largest instance) and finds more objects compared to baselines without a resolution hierarchy, as the search space becomes larger, and as the sensor uncertainty increases. We show that our approach enables a mobile robot to automatically find objects placed at different heights in two $10m^2 \times 2m$ regions by moving its base and actuating its torso.

I. INTRODUCTION

Robots operating in human spaces such as homes must find objects such as glasses, mobile phones, or cleaning supplies that could be on the floor, shelves, or tables. This search space is naturally 3D. For humans, finding objects is a frequent task that involves hypothesizing search regions (e.g. the kitchen or lounge corner) based on semantic knowledge or past experience [1, 2], but ultimately depends on careful search by moving and looking within a search region [3, 4]. Analogously for robots, finding objects requires the ability to produce an efficient search policy under limited field of view (FOV) within a designated search region, where target objects could be partially or completely occluded.

Unfortunately, searching for a single, static object by planning sensing parameters (e.g. position of the camera) in 3D is NP-complete [5]. Further complications arise due to sensor uncertainty or when multiple objects must be found. The Partially Observable Markov Decision Process (POMDP) [6] has been widely adopted as a framework to describe and optimally solve the object search problem [4, 7, 8], as it captures both uncertainty about the target location and the on-board sensors. However, to ensure the POMDP is manageable to solve, previous works often reduce the search space or robot mobility to 2D [2, 3, 9]. The key challenges lie in the intractability of maintaining exact belief due to large state space [10], and the high branching factor for planning due to large observation space [11, 12].

We introduce the 3D multi-object search (3D-MOS) task, a POMDP with 3D state and action spaces, and a realistic observation space in the form of labeled voxels within the

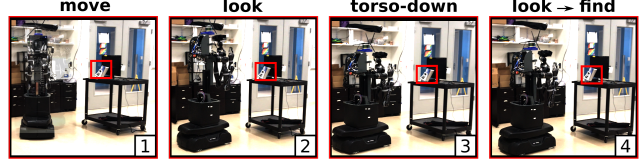


Fig. 1: Our approach enables a mobile robot to autonomously plan to lower its torso to search for a target object (marked by the red box). Action sequence: (1) MOVE which moves the robot base to be facing table, (2) then LOOK which observes free space due to a high torso. (3) The robot then decides to lower its torso, (4) LOOK again in the same direction, and finally FIND to mark the object as found. See supplementary video for footage.

viewing frustum from a mounted camera. Following Wandzel et al. [3], objects are assumed to be independent, allowing the belief space to scale linearly instead of exponentially in the number of objects. We address the challenges of computational complexity by developing several techniques that converge to an online multi-resolution planning algorithm. First, we propose a per-voxel observation model which drastically reduces the size of the observation space necessary for planning. Next, we present a novel octree-based belief representation that captures beliefs at different resolutions and allows efficient and exact belief updates. Then, we exploit the octree structure and derive *abstractions* of the ground problem at different resolution levels leveraging abstraction theory for MDPs [13, 14]. Finally, a Monte-Carlo Tree Search (MCTS) based algorithm, called Partially-Observable UCT [10], is employed to solve these abstract instances in parallel, and the action with highest value in its MCTS tree is selected for execution.

We evaluate our method in a simulated, discretized 3D domain where a robot with a 6 degrees-of-freedom camera searches for objects of different shapes and sizes randomly generated and placed in a grid world. The results show that our approach significantly outperforms the baselines without resolution hierarchy and abstraction as problem size scales and under different levels of sensor uncertainty. We further implement our approach on a torso-actuated mobile robot (Figure 1). The robot finds multiple objects in two $10m^2 \times 2m$ regions placed at different heights.

II. BACKGROUND

POMDPs compactly represent the robot’s uncertainty in target locations and its own sensor [6], and OO-POMDPs factor the domain in terms of objects, which fits the object search problem naturally [3]. Below, we first provide a brief overview of POMDPs and OO-POMDPs. Then, we discuss related work in object search.

¹Brown University, Providence, RI. ²MIT CSAIL, Cambridge, MA.
Email: {kzheng10, gdk, stefie10}@cs.brown.edu, yooncs8@csail.mit.edu

A. POMDPs and OO-POMDPs

A POMDP models a sequential decision making problem where the environment state is not fully observable by the agent. It is formally defined as a tuple $\langle \mathcal{S}, \mathcal{A}, \mathcal{O}, T, O, R, \gamma \rangle$, where $\mathcal{S}, \mathcal{A}, \mathcal{O}$ denote the state, action and observation spaces, and the functions $T(s, a, s') = \Pr(s'|s, a)$, $O(s', a, o) = \Pr(o|s', a)$, and $R(s, a) \in \mathbb{R}$ denote the transition, observation, and reward models. The agent takes an action $a \in \mathcal{A}$ and causes the environment state to transition from $s \in \mathcal{S}$ to $s' \in \mathcal{S}$. The environment in turn returns the agent an observation $o \in \mathcal{O}$ and reward $r \in \mathbb{R}$. A *history* $h_t = (ao)_{1:t-1}$ captures all past actions and observations. The agent maintains a distribution over states given current history $b_t(s) = \Pr(s|h_t)$. The agent updates its belief after taking an action and receiving an observation by $b_{t+1}(s') = \eta \Pr(o|s', a) \sum_s \Pr(s'|s, a) b_t(s)$ where η is the normalizing constant. The task of the agent is to find a policy $\pi(b_t)$ which maximizes the expectation of future discounted rewards with a discount factor γ .

An OO-POMDP [3] (generalization of OO-MDP [15]) is a POMDP that considers the state and observation spaces to be factored by a set of n objects. A simplifying assumption that objects are independent is made for the 2D MOS domain [3] so that the belief space size grows linearly rather than exponentially in number of objects, namely, $b_t(s) = \prod_i b_t^i(s_i)$.

Offline POMDP solvers are often too slow to be practical for large domains [16]. State-of-the-art online POMDP solvers leverage sparse belief sampling and MCTS to scale to address the curse of history [10, 17, 18]. POMCP [10] is one such algorithm which combines particle belief representation with Partially Observable UCT (POUCT), which extends the UCT algorithm [19] to POMDPs and is proven to be asymptotically optimal [10]. We build upon POUCT due to its optimality and simplicity of implementation.

B. Related Work

Previous work primarily address the computational complexity of object search by hypothesizing likely regions based on object co-occurrence [1], semantic knowledge [2] or language [3], reducing the state space from 3D to 2D [3, 20, 21, 22], or constrain the sensor to be stationary [8, 23]. Our work focuses on multi-object search within a 3D region where the robot actively moves the mounted camera, for example, through pan or tilt, or by moving itself.

Several works explicitly reason over the arrangement of occluded objects based on given geometry models of clutter [4, 22, 24]. Our approach considers occlusion as part of the observation that contains no information about target locations and we do not require geometry models.

Many works formulate object search as a POMDP. Notably, Aydemir et al. [2] first infer a room to search in then perform search by calculating candidate viewpoints in a 2D plane. Li et al. [9] plan sensor movements online, yet assume objects are placed at the same surface level in a container with partial occlusion. Xiao et al. [4] address object fetching on a cluttered tabletop where the robot's FOV fully covers the scene, and that occluding obstacles are removed

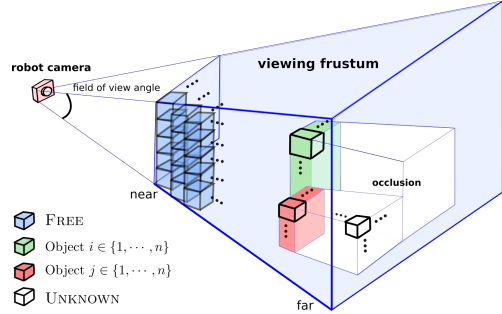


Fig. 2: Illustration of the viewing frustum and volumetric observation. The viewing frustum V consists of $|V|$ voxels, where each $v \in V$ can be labeled as $i \in \{1, \dots, n\}$, FREE or UNKNOWN.

permanently during search. Wandzel et al. [3] formulates the multi-object search (MOS) task on a 2D map using the proposed Object-Oriented POMDP (OO-POMDP). We extend that work to 3D and tackle additional challenges by proposing a new observation model and belief representation, and a multi-resolution planning algorithm. In addition, our POMDP formulation allows fully occluded objects and can be in principle extended to different robots such as mobile robots or drones.

III. MULTI-OBJECT SEARCH IN 3D

The robot is tasked to search for n static target objects (e.g. cup and book) of known type but unknown location in a search space that also contains static non-target obstacles. We assume the robot is able to localize itself and navigate between locations. We also assume it has access to detectors for the objects that it is searching for. The search space is a discretized 3D grid world denoted by G . We introduce the 3D-MOS domain as an OO-POMDP as follows:

State space \mathcal{S} . A state is defined as $s = \{s_1, \dots, s_n, s_r\}$:

- $s_i = g \in \mathcal{S}_i$ is the location of *target object* i where $g \in G$ indicates the 3D pose at its center of mass.
- $s_r = (p, \mathcal{F}) \in \mathcal{S}_r$ is the state of the *robot* where p is the 6D camera pose and \mathcal{F} is the set of found objects.

Observation space \mathcal{O} . An observation is defined as $o = \{(v, d(v))|v \in V\}$, where V is the viewing frustum that represents the FOV (Figure 2), and $d(v)$ is a *detection function* that labels the voxel $v \in V$ to be either an object $i \in \{1, \dots, n\}$, FREE or UNKNOWN. FREE denotes that the voxel is a free space or an obstacle. UNKNOWN denotes an unknown region due to occlusion incurred by target objects or static obstacles. We let $V \subseteq G$ for notational convenience, but in general a voxel with higher resolution can be easily mapped to a corresponding grid cell.

We can decompose V by objects into V_1, \dots, V_n where for any $v \in V_i$, $d(v) \in \{i, \text{FREE}\}$ which retain the same information as V for a given robot state.¹ Hence, the observation o can be factored by objects such that $o = \bigcup_{i=1}^n o_i$ where $o_i = \{(v, d(v))|v \in V_i\}$.

Action space \mathcal{A} and transition function T . There are three types of primitive actions: $\text{MOVE}(s_r, g)$ action moves

¹The FOV V is fixed for a given camera pose in the robot state, therefore excluding UNKNOWN voxels does not lose information.

the robot from pose in s_r to destination $g \in G$. $\text{LOOK}(\theta)$ changes the camera pose to look in the direction specified by $\theta \in \mathbb{R}^3$, and projects a viewing frustum V . $\text{FIND}(i, g)$ declares object i to be found at location g . The implementation of these actions may vary depending on the type of search space or robot. All transitions are assumed to be deterministic.

Reward function R . The robot receives $+1000$ if an object is correctly identified by a FIND action, otherwise the FIND action incurs a -1000 penalty. MOVE and LOOK actions receive a step cost of -1 ; MOVE receives an additional penalty based on the distance traveled.

A. Observation Model

Generative modeling of 3D geometry is challenging, and previous methods involve inference processes costly for practical POMDP planning [25]. To develop an efficient model, we make the simplifying assumption that object i is contained within a single voxel located at the grid cell $g = s'_i$. We address the case of searching for objects of unknown sizes with our planning algorithm (Section V) that plans at multiple resolutions in parallel.

Thus, $d(v) = \text{FREE}$ deterministically for $v \neq s'_i$, and the uncertainty of o_i is reduced to the uncertainty of $d(s'_i)$. We can therefore approximate $\Pr(o_i|s', a)$ by $\Pr(d(s_i)|s', a)$. When $s'_i \in V_i$, that is, the non-occluded region covers s'_i , the case of $d(s'_i) = i$ indicates correct detection (true positive) while $d(s'_i) = \text{FREE}$ indicates sensing error (false negative). We let $\Pr(d(s'_i) = i|s', a) = \alpha$ and $\Pr(d(s'_i) = \text{FREE}|s', a) = \beta$. When $s'_i \notin V_i$, either $d(s'_i) = \text{UNKNOWN}$ (occlusion) or $s'_i \notin V$ (not in FOV). In this case, there is no information regarding the value of $d(s'_i)$ in the observation o_i , therefore $\Pr(d(s'_i)|s', a)$ is a uniform distribution. Therefore, α and β are the parameters which control the true positive and false negative rates of the detector. Note that the belief update equation does not require the observation model to be normalized as normalization is handled by η (See Section II-A).

IV. OCTREE BELIEF REPRESENTATION

Particle belief representation [10, 17] suffers particle depletion under large observation spaces. Moreover, if the resolution of G is dense, it may be possible that most of 3D grid cells do not contribute to the behavior of the robot.

We represent a belief state $b_t^i(s_i)$ for object i as an *octree*. An octree is a tree where every node has 8 children. In our context, a node represents a grid cell $g^l \in G^l$, where l is the resolution level, such that g^l covers a cubic volume of $(2^l)^3$ ground-level grid cells; the ground resolution level is given by $l = 0$. The 8 children of the node equally subdivide the volume at g^l into smaller volumes at resolution level $l - 1$ (Figure 3). Each node has a value $\text{VAL}_t^i(g^l) \in \mathbb{R}$, which represents the unnormalized belief that $s_i^l = g^l$, that is, object i is located at grid cell g^l . We denote the set of nodes at resolution level $k < l$ that reside in a subtree rooted at g^l by $\text{CH}^k(g^l)$. By definition, $b_t^i(g^l) = \Pr(g^l|h_t) = \sum_{c \in \text{CH}^k(g^l)} \Pr(c|h_t)$. Thus, with a normalizer

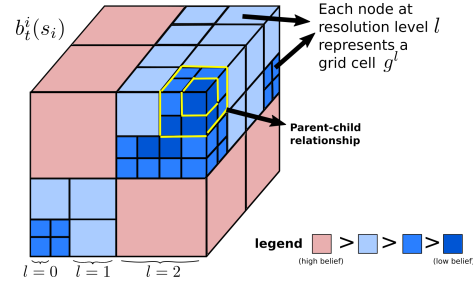


Fig. 3: Illustration the octree belief representation $b_t^i(s_i)$. The color on a node g^l indicates the belief $\text{VAL}_t^i(g^l)$ that the object is located within g^l . The highlighted grid cells indicate parent-child relationship between a grid cell at resolution level $l = 1$ (parent) and one at level $l = 0$.

$\text{NORM}_t = \sum_{g \in G} \text{VAL}_t^i(g)$, we can rewrite the normalized belief as:

$$b_t^i(g^l) = \frac{\text{VAL}_t^i(g^l)}{\text{NORM}_t} = \sum_{c \in \text{CH}^k(g^l)} \left(\frac{\text{VAL}_t^i(c)}{\text{NORM}_t} \right), \quad (1)$$

which means $\text{VAL}_t^i(g^l) = \sum_{c \in \text{CH}^k(g^l)} \text{VAL}_t^i(c)$.

The octree does not need to be constructed fully in order to query the probability at any grid cell. This can be achieved by setting a default value $\text{VAL}_0^i(g) = 1$ for all ground grid cells $g \in G$ not yet present in the octree. Then, any node corresponding to g^l has a default value of $\text{VAL}_0^i(g^l) = \sum_{c \in \text{CH}^1(g^l)} \text{VAL}_0^i(c) = |\text{CH}^1(g^l)|$.

We refer to this belief state representation as *octree belief*. It can yield the belief of object state at different resolution levels. Next, we describe the belief update and sampling algorithm for the octree belief representation.

A. Belief Update

We have defined a per-voxel observation model for $\Pr(o_i|s', a)$ which reduces o_i to $d(s'_i)$ if $s'_i \in V_i$, or is a uniform distribution if $s'_i \notin V_i$. This suggests that the belief update need only happen for voxels that are inside the FOV to reflect the information in the observation.

Upon receiving observation o_i within the FOV V_i , belief is updated according to Algorithm 1. This algorithm updates the value of the ground-level node g corresponding to each voxel $v \in V_i$ as $\text{VAL}_{t+1}^i(g) = \Pr(d(v)|s', a) \text{VAL}_t^i(g)$. The normalizer is updated to make sure b_{t+1}^i is normalized

Lemma 1: The normalizer NORM_t at time t can be correctly updated by adding the incremental update of values as in Algorithm 1.

Proof: We begin by applying the definition of the normalizer at time $t + 1$, $\text{NORM}_{t+1} = \sum_{s_i \in G} \text{VAL}_{t+1}^i(s_i)$. We can decompose this sum into two cases where the object i is inside of V_i and outside of V_i ; For object locations $s_i \notin V_i$, the *unnormalized* observation model is uniform, thus $\text{VAL}_{t+1}^i(s_i) = \Pr(d(s_i)|s', a) \text{VAL}_t^i(s_i) = \text{VAL}_t^i(s_i)$. Therefore, $\text{NORM}_{t+1} = \sum_{s_i \in V_i} \text{VAL}_{t+1}^i(s_i) + \sum_{s_i \notin V_i} \text{VAL}_t^i(s_i)$. Note the set $\{s_i | s_i \notin V_i\}$ is equivalent as $\{s_i | s_i \in G \setminus V_i\}$. Using this fact and the definition of NORM_t , we obtain $\text{NORM}_{t+1} = \text{NORM}_t + \sum_{s_i \in V_i} (\text{VAL}_{t+1}^i(s_i) - \text{VAL}_t^i(s_i))$ which proves the lemma. ■

Algorithm 1: OctreeBeliefUpdate $(b_t^i, a, o_i) \rightarrow b_{t+1}^i$

input : b_t^i : octree belief for object i ; a : action taken by robot; $o_i = \{(v, d(v)) | v \in V_i\}$: factored observation for object i

output: b_{t+1}^i : updated octree belief

// Let $\Psi(b_t^i)$ denote the octree underlying b_t^i .

for $v \in V_i$ **do**

$s_i \leftarrow v$; // State $s_i \in G$ at grid cell corresponding to voxel v

if $g \notin \Psi(b_t^i)$ **then**

| Insert node at g to $\Psi(b_t^i)$;

end

$\text{VAL}_{t+1}^i(s_i) \leftarrow \Pr(d(v)|s', a) \text{VAL}_t^i(s_i);$

$\text{NORM}_{t+1} \leftarrow \text{NORM}_t + \text{VAL}_{t+1}^i(s_i) - \text{VAL}_t^i(s_i);$

end

This belief update is therefore *exact* since the transition function is deterministic. The complexity of this algorithm is $O(|V| \log(|G|))$; Inserting nodes and updating values of nodes can be done by traversing the tree depth-wise.

B. Sampling

Octree belief affords exact belief sampling at any resolution level in logarithmic time complexity with respect to the size of the search space $|G|$, despite not being completely built. Given resolution level l , we sample from \mathcal{S}_i^l by traversing the octree in a depth-first manner. Let l_{\max} denote the maximum resolution level for the search space. Let l_{des} be the *desired* resolution level at which a state is sampled. If $s_i^{l_{\text{des}}}$ is sampled, then all nodes in the octree that cover $s_i^{l_{\text{des}}}$, i.e., $s_i^{l_{\max}}, \dots, s_i^{l_{\text{des}}+2}, s_i^{l_{\text{des}}+1}$, must also be implicitly sampled. Also, the event that s_i^{l+k} is sampled is independent from other samples given that s_i^{l+k+1} is sampled. Hence, the task of sampling $s_i^{l_{\text{des}}}$ is translated into sampling a sequence of samples $s_i^{l_{\max}}, \dots, s_i^{l_{\text{des}}+2}, s_i^{l_{\text{des}}+1}, s_i^{l_{\text{des}}}$, each according to the distribution $\Pr(s_i^l | s_i^{l+1}, h_t) = \frac{\text{VAL}_t^i(s_i^l)}{\text{VAL}_t^i(s_i^{l+1})}$. Sampling from this probability distribution is efficient, as the sample space, i.e. the children of node s_i^{l+1} is only of size 8. Therefore, this sampling scheme yields a sample $s_i^{l_{\text{des}}}$ exactly according to $b_t^i(s^{l_{\text{des}}})$ with time complexity $O(\log(|G|))$.

V. MULTI-RESOLUTION PLANNING VIA ABSTRACTIONS

POUCT expands an MCTS tree using a *generative function* $(s', o, r) \sim \mathcal{G}(s, a)$, which is straightforward to acquire since we explicitly define the 3D-MOS models. However, directly applying POUCH is subject to high branching factor due to the large observation space in our domain.

Our intuition is that the resolution hierarchy encoded in octree belief naturally imposes a spatial state abstraction, which can be used to derive a corresponding abstract observation space used for planning. We first formulate an *abstract 3D-MOS* which has smaller state and observation spaces compared to the ground 3D-MOS. We then motivate and describe our multi-resolution planning algorithm.

A. Abstract 3D-MOS

We adopt the abstraction scheme in Li et al. [13] where in general, the abstract transition and reward functions are weighted sums of the original problem's transition and reward functions, respectively where the weights sum up to 1. We define an abstract 3D-MOS $\langle \hat{\mathcal{S}}, \hat{\mathcal{A}}, \hat{\mathcal{O}}, \hat{T}, \hat{O}, R, \gamma, l \rangle$ at resolution level l as follows.

State space $\hat{\mathcal{S}}$. For each object i , an abstraction function $\phi_i : \mathcal{S}_i \rightarrow \mathcal{S}_i^l$ transforms the ground-level object state s_i to an abstract object state s_i^l at resolution level l . The abstraction of the full state is $\hat{s} = \phi(s) = \{s_r\} \cup \bigcup_i \phi_i(s_i)$ where the robot state s_r is kept as is. The *inverse image* $\phi_i^{-1}(s_i^l)$ is the set of ground states that correspond to s_i^l under ϕ_i [13].

Action space $\hat{\mathcal{A}}$. Since state abstraction lowers the resolution of the search space, we consider macro move actions that moves the robot over longer distance at each planning step. Each macro move action $\text{MOVEOP}(s_r, g)$ is an *option* [26] that moves s_r to goal location g using multiple MOVE actions. The primitive LOOK and FIND actions are kept.

Transition function \hat{T} . Targets and obstacles are still static, and the robot still moves deterministically. However, the transition of the found set from \mathcal{F} to \mathcal{F}' is special since the action FIND(i, g) operates at the ground level while s_i^l has a lower resolution ($l > 0$). Let f_i be the binary state variable that is true if and only if object $i \in \mathcal{F}$. Because the action FIND(i, g) affects f_i based only on whether object i is located at g , and that the problem is no longer Markovian due to state abstraction [14], f_i transitions to f'_i following

$$\Pr(f'_i | f_i, s_i^l, h_t, \text{FIND}(i, g)) \quad (2)$$

$$= \sum_{s_i \in \phi_i^{-1}(s_i^l)} \Pr(f'_i | s_i, f_i, \text{FIND}(i, g)) \Pr(s_i | s_i^l, h_t). \quad (3)$$

The above is consistent with the abstract transition function in the works [13, 14] where the first term corresponds to the ground-level deterministic transition function and the second term $\Pr(s_i | s_i^l, h_t)$, stored in the octree belief, is the *weight* that sums up to 1 for all $s_i \in \mathcal{S}_i$.

Observation space $\hat{\mathcal{O}}$ and function \hat{O} . For the purpose of planning, we again use the assumption that an object is contained within a single voxel (yet at resolution level l). Then, given state \hat{s}' , the abstract observation o_i^l is regarded as a voxel-label pair $(s_i^l, d(s_i^l))$. Since it is computationally expensive to sum out all object states, we approximate the observation model by ignoring objects other than i :

$$\Pr(o_i^l | \hat{s}', a, h_t) = \Pr(d(s_i^l) | \hat{s}', a, h_t) \quad (4)$$

$$\approx \Pr(d(s_i^l) | s_i^l, s_r, a, h_t) \quad (5)$$

$$= \sum_{s_i \in \phi_i^{-1}(s_i^l)} \Pr(d(s_i^l) | s_i, s_r, a) \Pr(s_i | s_i^l, h_t). \quad (6)$$

This resembles the abstract transition function, where $\Pr(d(s_i^l) | s_i, s_r, a)$ is the ground observation function, and $\Pr(s_i | s_i^l, h_t)$ is the weight.

Reward function R . The reward function is the same as the one in ground 3D-MOS, since computing the reward only depends on the robot state which is not abstracted and the abstract action space consists of the same primitive actions as

Algorithm 2: MR-POUCT $(\mathcal{P}, b_t, d) \rightarrow \hat{a}$

input : \mathcal{P} : a set of abstract 3D-MOS instances at different resolution levels; b_t : belief at time t ; d : planning depth

output: \hat{a} : an action in the action space of some $P_t \in \mathcal{P}$

procedure $\text{Plan}(b_t)$

```

foreach  $P_t \in \mathcal{P}$  in parallel do
    // Recall that  $P_t = \langle \hat{\mathcal{S}}, \hat{\mathcal{A}}, \hat{\mathcal{O}}, \hat{T}, \hat{\mathcal{O}}, R, \gamma, l \rangle$ 
     $\mathcal{G} \leftarrow \text{GenerativeFunction}(P_t);$ 
     $Q_P(b_t, \hat{a}) \leftarrow \text{POUCT}(\mathcal{G}, h_t, d);$ 
end
 $\hat{a} \leftarrow \text{argmax}_{\hat{a}} \{Q_P(b_t, \hat{a}) | P \in \mathcal{P}\};$ 
return  $\hat{a}$ 

```

3D-MOS. Therefore, solving an abstract 3D-MOS is solving the same task as the original 3D-MOS.

B. Multi-Resolution Planning Algorithm

Abstract 3D-MOS is smaller than the original 3D-MOS which may provide benefit in online planning. However, it may be difficult to define a single resolution level, due to the uncertainty of the size or shape of objects, and the unknown distance between the robot and these objects.

Therefore, we propose to solve a number of abstract 3D-MOS problems in parallel, and select an action from $\hat{\mathcal{A}}$ with the highest value for execution. The algorithm is formally presented in Algorithm 2. The set of abstract 3D-MOS problems, \mathcal{P} , can be defined based on the dimensionality of the search space and the particular object search setting. Then, it is straightforward to define a *generative function* $\mathcal{G}(\hat{s}, \hat{a}) \rightarrow (\hat{s}', \hat{o}, r)$ from an abstract 3D-MOS instance P using its transition, observation and reward functions. POUCT uses \mathcal{G} to build a search tree and plan the next action. Thus, all problems in \mathcal{P} are solved online in parallel, each by a separate POUCT. The final action with the highest value ($Q_P(b_t, \hat{a})$) in its respective POUCT search tree is chosen as the output (see [10] for details on POUCT). We call this algorithm Multi-Resolution POUCT (MR-POUCT).

VI. EXPERIMENTS

We assess the hypothesis that our approach, MR-POUCT, improves the robot's ability to efficiently and successfully find objects especially in large search spaces. We conduct a simulation evaluation and a study on the real robot.

A. Simulation Evaluation

We implement our approach in a simulated environment designed to reflect the essence of the 3D-MOS domain (Figure 4). Each simulated problem instance is defined by a tuple (m, n, d) , where the search region G has size $|G| = m^3$ with n randomly generated, randomly placed objects. The on-board camera that projects a viewing frustum with 45 degree FOV angle, an 1.0 aspect ratio, a minimum range of 1 grid cell, and a maximum range of d grid cells. Hence, we can increase the difficulty of the problem by increasing

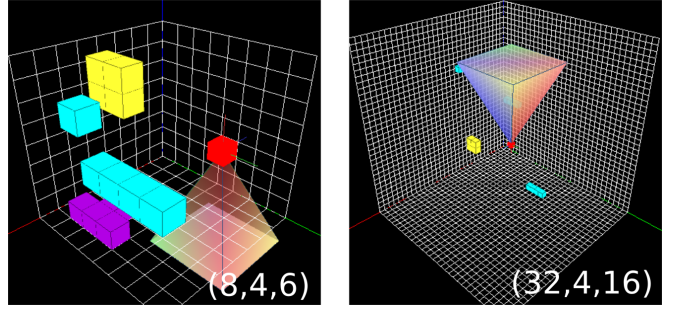


Fig. 4: Simulated environment for 3D object search. The robot (represented as a red cube) can project a viewing frustum to observe the search space, where objects are represented by sets of cubes. Search space size scales from 4^3 to 32^3 . The tuple (m, n, d) at lower-right defines the problem instance.

m and n , or by reducing the percentage of voxels covered by a viewing frustum through reducing the FOV range d . Occlusion is simulated using perspective projection and treating each grid cell as a point.

There are two primitive MOVE actions per axis (e.g. $+z$, $-z$) that each moves the robot along that axis by one grid cell. There are two LOOK actions per axis, one for each direction. Finally, a FIND action is defined that declares all not-yet-found objects within the viewing frustum as found. Thus, the total number of primitive actions is 13. If multiple new objects are present within one viewing frustum when the FIND is taken, only the maximum reward of +1000 is provided. The task terminates either when the total planning time limit is reached or n FIND actions are taken.

We compare our approach (MR-POUCT) with the following baselines. The first baseline is the original POUCT [10] which solves the ground POMDP directly without using resolution hierarchy in the octree belief. The second baseline (Options+POUCT) is an ablation where only the motion action abstraction (i.e. MOVEOP options) is used. This means the robot can plan to move at larger step sizes, but does not consider spatial state or observation abstraction and only has access to ground-level belief. Additionally, POMCP is used to demonstrate the impact of particle deprivation on planning. As a lower bound, we use PO-Rollout, used also in Silver and Veness [10], which chooses actions by sampling from a random rollout policy instead of constructing a search tree.

Each algorithm begins with uniform prior and is allowed a maximum of 3.0s for planning each step. The total amount of allowed planning time *plus* time spent on belief update is 120s, 240s, 360s, and 480s for environment sizes (m) of 4, 8, 16, or 32, respectively. We set discount factor $\gamma = 0.99$. For each (m, n, d) setting, 40 trials (with random world generation) are conducted.

Results. We evaluate the *scalability* of our approach with 4 different settings of search space size $m \in \{4, 8, 16, 32\}$ and 3 settings of number of objects $n \in \{2, 4, 6\}$, resulting in 12 combinations. The FOV range d is chosen such that the percentage of the grids covered by one projection of the viewing frustum *decreases* as the world size m increases². The sensor

²The maximum FOV coverage for $m = 4, 8, 16$, and 32 is 17.2% ($d = 4$), 8.8% ($d = 6$), 4.7% ($d = 10$), and 2.6% ($d = 16$), respectively.

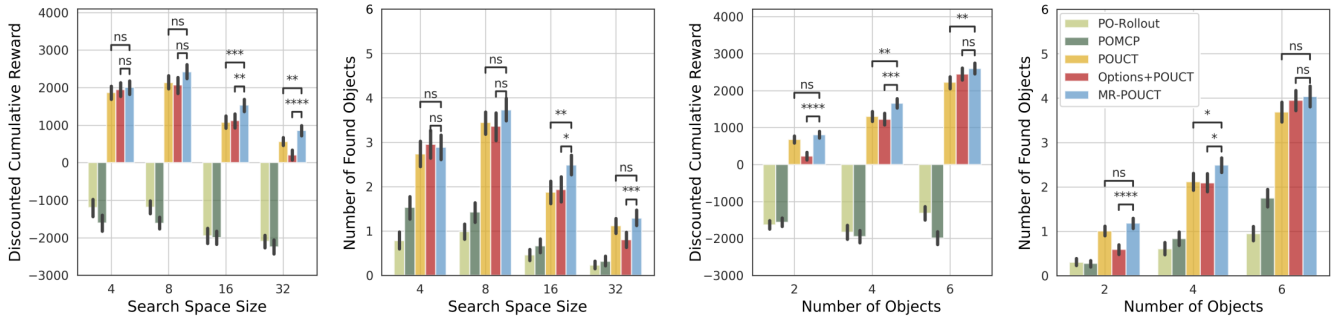


Fig. 5: Discounted cumulative reward and number of found objects as the search space increases, and as the number of total objects increases. The results for each search space size (m) is obtained by aggregating over all number of objects (n) settings, and vice versa. The level of statistical significance is indicated by ns ($p > 0.05$), * ($p \leq 0.05$), ** ($p \leq 0.01$), *** ($p \leq 0.001$), **** ($p \leq 0.0001$).

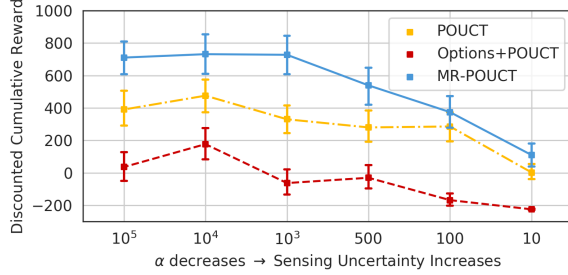


Fig. 6: Discounted cumulative reward with 95% confidence interval as the sensing uncertainty increases, aggregating over the β settings.

is assumed to be near-perfect, with $\alpha = 10^5$ and $\beta = 0$ (recall that α and β correspond to the true positive and false negative rate of the sensor). Results are shown in Figure 5. Particle deprivation happens quickly due to large observation space, and the behavior degenerates to a random agent as in [10, 3], causing POMCP to perform poorly. MR-POUCT is competitive against the two POUCT variants when the search space is small, and outperforms them significantly as the search space scales. When the search space contains fewer objects, MR-POUCT and POUCT show more resilience than Options+POUCT, with MR-POUCT performing consistently better on average. We observe that the gain of MR-POUCT in discounted reward is more significant than that in the number of found objects, which suggests it can produce more efficient search policies. This demonstrates the benefit of planning with the resolution hierarchy in octree belief.

We then investigate the performance of our method with respect to changes in sensing uncertainty, controlled by the parameters α and β of the observation model. According to the belief update algorithm in Section IV-A, a noisy but functional sensor should increase the belief $VAL_t^i(g)$ for object i if an observed voxel at g is labeled i , while decrease the belief if labeled FREE. This implies that a properly working sensor should satisfy $\alpha > 1$ and $\beta < 1$. We investigate on 5 settings of $\alpha \in \{10, 100, 500, 10^3, 10^4, 10^5\}$ and 2 settings of $\beta \in \{0.3, 0.8\}$. A fixed problem difficulty of (16, 2, 10) is used to conduct this experiment. Results in Figure 6 show that MR-POUCT is consistently better in all parameter settings. We observe that β has almost no impact to any algorithm's performance as long as $\beta < 1$, whereas decreasing α changes the agent behavior such that it must decide to LOOK multiple times before being certain.

B. Demonstration on a Torso-Actuated Mobile Robot

We demonstrate that our approach is scalable to real world settings by implementing the 3D-MOS problem as well as MR-POUCT for a mobile robot setting. We use the Kinova MOVO Mobile Manipulator robot, which has an actuated torso that can raise up to around 0.5m and lower down to around 0.05m, which facilitates a 3D action space. The robot operates in a lab environment, which is decomposed into two *search regions* G_1 and G_2 of size roughly $10m^2 \times 2m$ (Figure. 1), each with a semantic label (“shelf-area” for G_1 and “whiteboard-area” for G_2). The robot is tasked to look for n_{G_1} and n_{G_2} objects in each search region sequentially, where objects are represented by paper AR tags that could be in clutter or not detectable at an angle. The robot instantiates an instance of the 3D-MOS problem once it navigates to a search region. In this 3D-MOS implementation, the MOVE actions are implemented based on a topological graph on top of a metric occupancy grid map. The neighbors of a graph node form the motion action space when the robot is at that node. The robot can take LOOK action in 4 cardinal directions in place and receive volumetric observations; A volumetric observation is a result of downsampling and thresholding points in the corresponding point cloud. The robot was able to find 3 out of 5 total objects in the two search regions in around 15 minutes. One sequence of actions (Figure 1) show that the robot decides to lower its torso in order to LOOK and FIND an object. Supplementary video contains the footage with visualization of the volumetric observation and octree belief update.

VII. CONCLUSION

We present a POMDP formulation of multi-object search in 3D with volumetric observation space and solve it with a novel multi-resolution planning algorithm. Our evaluation demonstrates that such challenging POMDPs can be solved online efficiently and scalably with practicality for real robot by extending existing general POMDP solvers with domain-specific structure and belief representation. One limitation of our work is that we do not explicitly reason over object geometry. One direction of future work is to investigate belief filtering techniques based on shape priors to more accurately maintain the belief over possible target locations.

REFERENCES

[1] Thomas Kollar and Nicholas Roy. Utilizing object-object and object-scene context when planning to find things. In *IEEE International Conference on Robotics and Automation*, pages 2168–2173. IEEE, 2009.

[2] Alper Aydemir, Andrzej Pronobis, Moritz Göbelbecker, and Patric Jensfelt. Active visual object search in unknown environments using uncertain semantics. *IEEE Transactions on Robotics (T-RO)*, 29(4):986–1002, August 2013. doi: 10.1109/TRO.2013.2256686.

[3] Arthur Wandzel, Yoonseon Oh, Michael Fishman, Nishanth Kumar, and Stefanie Tellex. Multi-object search using object-oriented POMDPs. In *2019 International Conference on Robotics and Automation (ICRA)*, pages 7194–7200. IEEE, 2019.

[4] Yuchen Xiao, Sammie Katt, Andreas ten Pas, Shengjian Chen, and Christopher Amato. Online planning for target object search in clutter under partial observability. In *Proceedings of the International Conference on Robotics and Automation*, 2019.

[5] Yiming Ye and John K Tsotsos. Sensor planning in 3d object search: its formulation and complexity. In *The 4th International Symposium on Artificial Intelligence and Mathematics, Florida, USA*. Citeseer, 1996.

[6] Leslie Pack Kaelbling, Michael L Littman, and Anthony R Cassandra. Planning and acting in partially observable stochastic domains. *Artificial intelligence*, 101(1-2):99–134, 1998.

[7] N. Atanasov, B. Sankaran, J. Le Ny, G. Pappas, and K. Daniilidis. Nonmyopic view planning for active object classification and pose estimation. *IEEE Trans. on Robotics (TRO)*, 30(5):1078–1090, 2014.

[8] Michael Danielczuk, Andrey Kurenkov, Ashwin Balakrishna, Matthew Matl, David Wang, Roberto Martín-Martín, Animesh Garg, Silvio Savarese, and Ken Goldberg. Mechanical search: Multi-step retrieval of a target object occluded by clutter. In *2019 International Conference on Robotics and Automation (ICRA)*, pages 1614–1621. IEEE, 2019.

[9] Jue Kun Li, David Hsu, and Wee Sun Lee. Act to see and see to act: POMDP planning for objects search in clutter. In *2016 IEEE/RSJ International Conference on Intelligent Robots and Systems (IROS)*, pages 5701–5707. IEEE, 2016.

[10] David Silver and Joel Veness. Monte-Carlo planning in large POMDPs. In *Advances in neural information processing systems*, pages 2164–2172, 2010.

[11] Zachary N. Sunberg and Mykel J. Kochenderfer. Online algorithms for POMDPs with continuous state, action, and observation spaces. Delft, 2018.

[12] Neha P Garg, David Hsu, and Wee Sun Lee. DESPOT- α : Online POMDP planning with large state and observation spaces. In *Robotics: Science and Systems*, 2019.

[13] Lihong Li, Thomas J Walsh, and Michael L Littman. Towards a unified theory of state abstraction for MDPs. In *ISAIM*, 2006.

[14] Aijun Bai, Siddharth Srivastava, and Stuart J Russell. Markovian state and action abstractions for MDPs via hierarchical mcts. In *IJCAI*, pages 3029–3039, 2016.

[15] Carlos Diuk, Andre Cohen, and Michael L Littman. An object-oriented representation for efficient reinforcement learning. In *Proceedings of the 25th international conference on Machine learning*, pages 240–247, 2008.

[16] Stéphane Ross, Joelle Pineau, Sébastien Paquet, and Brahim Chaib-Draa. Online planning algorithms for POMDPs. *Journal of Artificial Intelligence Research*, 32:663–704, 2008.

[17] Adhiraj Somani, Nan Ye, David Hsu, and Wee Sun Lee. DESPOT: Online pomdp planning with regularization. In *Advances in neural information processing systems*, pages 1772–1780, 2013.

[18] Zachary N Sunberg and Mykel J Kochenderfer. Online algorithms for POMDPs with continuous state, action, and observation spaces. In *International Conference on Automated Planning and Scheduling*, 2018.

[19] Levente Kocsis and Csaba Szepesvári. Bandit based Monte-Carlo planning. In *European conference on machine learning*, pages 282–293. Springer, 2006.

[20] Chaoqun Wang, Jiyu Cheng, Jiankun Wang, Xintong Li, and Max Q-H Meng. Efficient object search with belief road map using mobile robot. *IEEE Robotics and Automation Letters*, 3(4):3081–3088, 2018.

[21] Alejandro Sarmiento, Rafael Murrieta, and Seth A Hutchinson. An efficient strategy for rapidly finding an object in a polygonal world. In *Proceedings 2003 IEEE/RSJ International Conference on Intelligent Robots and Systems (IROS 2003)(Cat. No. 03CH37453)*, volume 2, pages 1153–1158. IEEE, 2003.

[22] Xinkun Nie, Lawson LS Wong, and Leslie Pack Kaelbling. Searching for physical objects in partially known environments. In *2016 IEEE International Conference on Robotics and Automation (ICRA)*, pages 5403–5410. IEEE, 2016.

[23] Mehmet R Dogar, Michael C Koval, Abhijeet Tallavajhula, and Siddhartha S Srinivasa. Object search by manipulation. *Autonomous Robots*, 36(1-2):153–167, 2014.

[24] Lawson LS Wong, Leslie Pack Kaelbling, and Tomás Lozano-Pérez. Manipulation-based active search for occluded objects. In *2013 IEEE International Conference on Robotics and Automation*, pages 2814–2819. IEEE, 2013.

[25] Jeong Joon Park, Peter Florence, Julian Straub, Richard Newcombe, and Steven Lovegrove. Deep sdf: Learning continuous signed distance functions for shape representation. In *Proceedings of the IEEE Conference on Computer Vision and Pattern Recognition*, pages 165–174, 2019.

[26] Richard S Sutton, Doina Precup, and Satinder Singh. Between MDPs and semi-MDPs: A framework for temporal abstraction in reinforcement learning. *Artificial intelligence*, 112(1-2):181–211, 1999.